

Spectroscopic and Mechanical Properties of Nano Silica Rubber Composite Material

Jung Kyu Lee¹, Juyun Park², Yong-Cheol Kang², and Sung Wi Koh^{1†}

Abstract

To manipulate the mechanical properties of acrylonitrile butadiene rubber (NBR), addition of nano-sized silica on rubber was performed and nano-silica NBR composite (NSR) materials were fabricated by press molding. The effect of volume fraction of silica in the NSR on the spectroscopic and mechanical properties has been studied.

Keywords: NBR, Nano-silica, Volume Fraction, NSR

1. Introduction

Polymer nano-composites (NCs) have been a subject of interest for their mechanical, chemical, and thermal properties instead of polymers and conventional composites materials. Before the use of polymer NCs to various components, such as rubber seals, bearings, and belts, in industrial materials^[1,2], the accurate analyses of their mechanical and chemical properties are necessary. The Charpy impact test is usually adopted to understand of polymer NCs for a long time, the relationship between the stress and the critical energy release rate has been considered important recently^[3-5].

Among various types of polymers, acrylonitrile butadiene rubber (NBR) is an attractive material system due to its excellent resistance to organic solvents^[6]. To improve the mechanical properties of NBR, the composites containing particles were introduced. The performance of composites is dependent on the particle size, volume fraction, and distribution of particles in the matrix^[7]. There is a large number of reports about the properties of NCs^[8-10]. NBR/clay NCs were prepared by melt blending method and exhibited excellent mechanical properties and thermal stability^[11]. Various particles are used for preparation of composites, silica

nano particle is one of promising additives. The mechanical properties of polystyrene/silica NCs in various silica contents were investigated. The NCs with less than 2% of silica shows the good performance about tensile, flexural, compressive strength, and impact and plain-strain fracture toughness^[12]. Because silica has hydroxyl group, it represents hydrophilic character. NBR also has hydrophilic group, C≡N bond, NBR and silica can be easily connected, and the effect of mixture may be show better performance than other NCs. However, the mechanical and spectroscopic study of NSRs was not reported yet.

The objectives of this study are to synthesize the NSR materials and to characterize the mechanical and chemical properties of the NSRs. The effect of volume fraction of silica on the mechanical properties, such as tensile strength, critical energy release rate, friction coefficient, and wear weight loss were investigated. Spectroscopic study is also performed to check the purity and the chemical environment of NSR materials.

2. Experimental Section

2.1. Preparation of NSR Materials

The mixture of NBR (N220S, JSR Co.) and nano-sized silica (UFP-30, average particle size of 99 nm, surface area of 30 m²/g, Denka) was prepared by press molding method. NBR is an unsaturated copolymer of acrylonitrile and butadiene and the structure of NBR is shown in Fig. 1. The molding process was carried out under temperature of 300°C, pressure of 20 bar, and

¹Department of Mechanical System Engineering, Pukyong National University, 365, Sinseon-Ro, Nam-Gu, Busan 48547, South Korea

²Department of chemistry, Pukyong National University, 45, Yongso-Ro, Nam-Gu, Busan 48513, South Korea

[†]Corresponding author : swkoh@pknu.ac.kr

(Received: January 18, 2016, Revised: March 15, 2016,

Accepted: March 25, 2016)

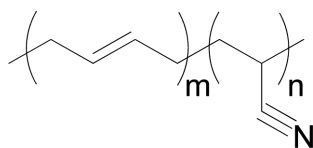


Fig. 1. Molecular structure of NBR.

holding time of 5 min. The volume fraction of silica was manipulated from 0.11 to 0.25.

The sample contains $xy\%$ of nano-silica on NBR will be denoted as NSR xy from here after.

2.2. Mechanical Tests

Tensile tests were performed at a constant crosshead speed of 5 mm/min and room temperature using electromechanical testing machine (ASC-1000G, capacity of 10 kN, Shimadzu). The test was conducted with the ASTM D638 (type I). Tensile specimens with same thickness as the supplied sheet (4.5 mm) were machined from the molded plates.

Notched Charpy impact tests were carried out on impact tester (Tinius Oslen Co. Max. Capacity 25 J) with an impact velocity of 3.46 m/s and a capacity of 20 J. Fig. 2 shows the details of the specimen used for impact test ($4.5 \times 10 \times 55 \text{ mm}^3$). After the production of notch in the center of the specimen using a cutter with thickness of 1 mm, the sharp notch was introduced by a fresh razor blade. The crack length was various from 1 to 2.25 mm and measured using a travel microscope (Pika Seiko LTD., 0.01 mm, X50). The temperature of the sample was maintained at 0 and -10°C using liquid nitrogen. From the results of impact test, the strain energy release rate, G_c is determined by the following equation.

$$U = U_k + G_c B W \phi \quad (1)$$

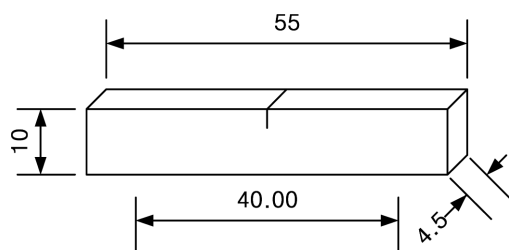


Fig. 2. Geometry of the specimen for Charpy impact test. The unit is mm.

where U is the strain energy, U_k is the kinetic energy, B is the thickness, W is the width, and ϕ is the compliance calibration factor which is influenced by the specimen geometry and notch dimensions. The slope from the plot of U verse $BW\phi$ indicates the G_c .

Dry sliding wear tests were performed using a pin-on-disc type tester at room temperature for each volume fraction of silica. The dimension of the specimen was $4.5 \times 5.5 \times 15 \text{ mm}^3$. Counter-part materials which is made of stainless steel with a diameter of 800 mm and an average roughness of $4 \mu\text{m}$ were prepared and cleaned with ethanol. Normal load was 10 N at a sliding velocity of 0.5 m/s. All sliding wear tests were carried out until 1000 m for each samples.

2.3. Chemical Properties

The chemical properties of NSR materials were characterized by X-ray photoelectron spectroscopy (XPS). Al $K\alpha$ source (1486.6 eV) and constant analyzer energy (CAE) mode were used for this study. The CAE, step size, and channeltron voltage of survey spectra were 100 eV, 0.5 eV, and 2500 V, respectively. High resolution spectra were obtained from CAE of 50 eV, step size of 0.05 eV, and other parameters are the same as survey spectra. The charge effect of spectra was adjusted by aliphatic carbon (284.6 eV).

3. Results and Discussion

Fig. 3 shows the tensile strength with respect to the volume fraction of silica. The volume fraction of silica increases from 0.11 to 0.25, the tensile strength is con-

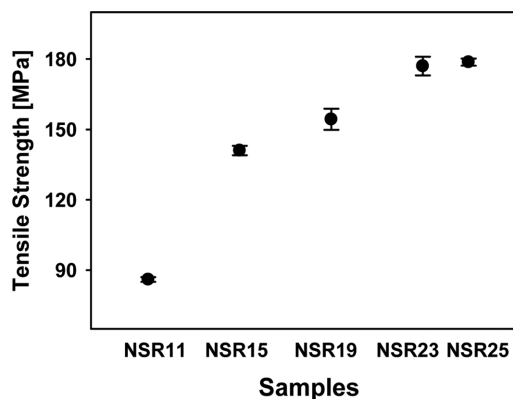


Fig. 3. Effect of silica content on the tensile strength of NSRs.

tinuously improved.

However, the increase range is gradually decreased, the volume fraction of silica is higher than 0.23, the tensile strength is almost constant. The addition of silica into NBR leads to the crosslink between NBR chains and improves the tensile strength. The increase of tensile strength is also observed the NCs of natural rubber and pristine clay^[13].

Fig. 4 shows the critical energy release rate as a function of volume fraction of silica at different temperature, 0 and -10°C. The critical energy release rate is obtained by equation (1). The volume fraction of silica is increased, the critical energy release rate is decreased. The phenomena is independent on the temperature, however, the change of critical energy release rate at 0°C is larger than that at -10°C. And the higher critical energy release rate is appeared at high temperature in the same volume fraction of silica. Thus, the highest value of critical energy release rate is 7.9 J/cm² at 0°C and 11% of silica. The change of critical energy release rate by temperature is caused by the difference in the coefficient of thermal expansion between NBR and silica. The coefficient of thermal expansion of NBR is about 10 times higher than that of silica^[14,15]. The NC materials with different coefficient of thermal expansions lies in the different states which is received by compressive or tensile stress of reinforcing particles at high or low temperature. At low temperature, the residual stress is increased, the critical energy release rate is decreased.

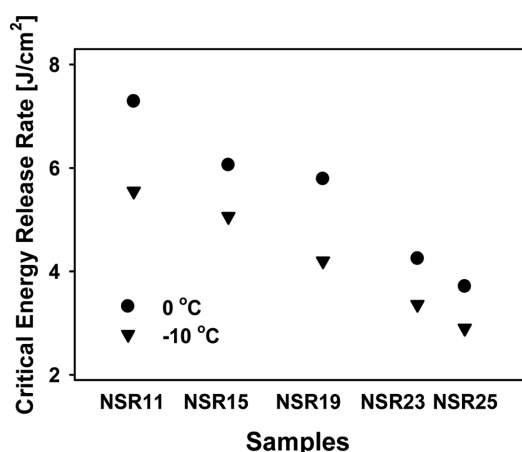


Fig. 4. Variation of critical energy release rate G_c with respect to 0°C and -10°C for various samples.

Fig. 5 shows the friction coefficient with various volume fraction of silica. The friction coefficient was generally reduced with the addition of silica. At the minor volume fraction of silica, the linear slope is appeared, however a great share of reduction in the friction coefficient was observed at the NSR containing silica of 0.25%. From the wear test, the information about variation of sample weight with different volume fraction of silica and distance was also obtained and shown in Fig. 6.

As the volume fraction of silica is increased, weight loss is decreased. The weight loss with same volume fraction of silica is increased with increasing the distance. At the 0.11 of volume fraction of silica, weight loss is 2.00×10^{-4} and 12.00×10^{-4} measured at the dis-

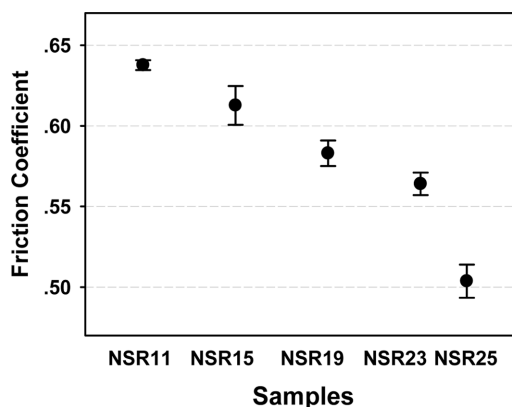


Fig. 5. Friction coefficient of NSR.

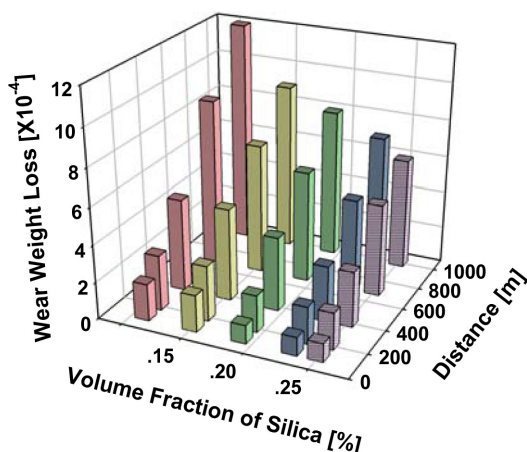


Fig. 6. Wear weight loss with the different volume fraction of silica and distance.

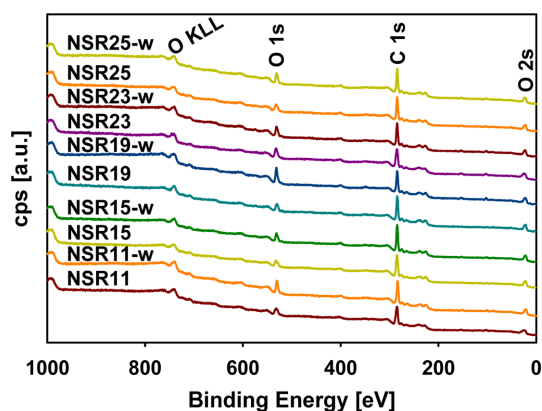


Fig. 7. Survey XPS spectra of NSRs.

tance of 100 and 1000 nm. The increase rate of weight loss is almost similar to all samples, such as NCs at the volume fraction of silica of 0.25 shows that the weight loss is raised to six times from 1.00×10^{-4} at 100 m to 6.00×10^{-4} at 1000 nm. These results are implied that the addition of silica in the NBR affects the mechanical properties of NSR.

Fig. 7 shows the survey spectra of NSRs. The sample name was summarized in volume fraction of silica and before or after wear test. NSR25-w sample indicates NBR with volume fraction of silica of 0.25 and after wear test, sample which has without w represents before wear test. From the survey spectra, several peaks appeared at about 743, 531, 285, and 23 eV. These peaks are assigned to carbon and oxygen peaks such as O KLL, O 1s, C 1s, and O 2s, respectively. And other atoms are not detected in survey spectra. This implies no impurities are included in NSRs. Comparing the samples before and after wear test, the peak intensities of C 1s is almost constant, but those of O 1s were changed. After the wear test, O 1s peaks are increased and it indicates NSRs are oxidized during the wear test.

For the better understanding of NSRs, the representative high resolution XPS spectra of O 1s, C 1s, and Si 2p are shown in Fig. 8 (a), (b), and (c), respectively. As mentioned in survey spectra, carbon peaks are not significantly different before and after wear test. However, the peak shapes of O 1s are different and the change is noticeably detected in high binding energy region at about 532 eV^[16]. It corresponds to oxygen bonded with silicon^[17]. As shown in Fig. 8 (c), the weak peaks of Si 2p at about 102 eV are evolved. In survey spectra, no

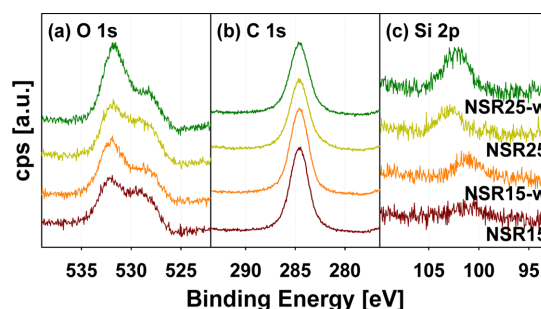


Fig. 8. High resolution XPS spectra of (a) O 1s, (b) C 1s, (c) and Si 2p.

peaks about Si are observed due to low volume fraction of silica. The peak intensity of NSR25 is higher than NSR15. The increase of volume fraction of silica in nano-composites can be verified by XPS. The peak position at about 102 eV is assigned to silicon oxide^[17]. Interestingly, the peak intensity of Si 2p is increased after wear test. It is confirmed that the content of silica in the surface region is increased after wear test and corresponded with O 1s spectra.

4. Conclusion

NBR and nano silica composites were prepared by press molding method. The mechanical properties, tensile, impact, and wear test were performed and chemical property was investigated with XPS. To control the properties of NCs, the volume fraction of silica in NSR was changed from 0.11 to 0.25. The purity of NCs and addition of silica were checked by XPS. And we could conclude that the increase of volume fraction of silica leads to the increase in the tensile strength and decrease in the critical energy release rate and friction coefficient.

Acknowledgement

This work was supported by Research Grant of Pukyong National University (CD2015-0613).

References

- [1] J. K. Lancaster, "Polymer-based bearing materials: The role of fillers and fibre reinforcement", *Tribology*, Vol. 5, pp. 249-255, 1972.
- [2] L. C. Vazquez, E. Hagel, B. J. Willenberg, W. Dai,

- F. Casanova, C. D. Batich, and M. Sartinorant, "Polymer-coated cannulas for the reduction of back-flow during intraparenchymal infusions", *J. Mater. Sci-Mater. M.*, Vol. 23, pp. 2037-2046, 2012.
- [3] J. R. Tarpani, O. Maluf, and M. C. A. Gatti, "Charpy impact toughness of conventional and advanced composite laminates for aircraft construction", *Materials Research*, Vol. 12, pp. 395-403, 2009.
- [4] H. W. Andresen and A. T. Echtermeyer, "Critical energy release rate for a CSM reinforced carbon fibre composite/steel bonding", *Compos. Part A-Appl. S.*, Vol. 37, pp. 742-751, 2006.
- [5] J. C. Slattery, K.-B. Fu, and E.-S. Oh, "The mechanics and thermodynamics of edge fracture: the critical energy release rate, the compatibility constraint, and the bond potential", *Philos. Mag.*, Vol. 92, pp. 1788-1802, 2012.
- [6] P. Yu, H. He, C. Jiang, Y. Jia, D. Wang, X. Yao, D. Jia, and Y. Luo, "Enhanced oil resistance and mechanical properties of nitrile butadiene rubber/lignin composites modified by epoxy resin", *J. Appl. Polym. Sci.*, Vol. 133, pp. 42922, 2016.
- [7] H. Kim, J. Kobashi, Y. Maeda, H. Yoshida, and M. Ozaki, "Pitch-length independent threshold voltage of polymer/cholesteric liquid crystal nano-composites", *Crystals*, Vol. 5, pp. 302-311, 2015.
- [8] M. Razavizadeh and M. Jamshidi, "Adhesion of nitrile rubber (NBR) to polyethylene terephthalate (PET) fabric. Part 1: PET surface modification by methylenediphenyl di-isocyanate (MDI)", *Appl. Surf. Sci.*, Vol. 360, pp. 429-435, 2016.
- [9] E. Kontou and G. Anthoulis, "The effect of silica nanoparticles on the thermomechanical properties of polystyrene", *J. Appl. Polym. Sci.*, Vol. 105, pp. 1723-1731, 2007.
- [10] S. H. Lee and Y. Choi, "Effect of nano-sized oxide particles on thermal and electrical properties of epoxy silica composites", *Phys. Met. Metallogr.*, Vol. 115, pp. 1295-1299, 2014.
- [11] R. L. Zhang, T. X. Li, Y. D. Huang, and L. Liu, "Effect of the clay on the thermal stability and mechanical properties of Nitrile-Butadiene Rubber (NBR)/clay nanocomposites", *J. Optoelectron. Adv. M.*, Vol. 16, pp. 629-633, 2014.
- [12] H. S. Vaziri, M. Abadyan, M. Nouri, I. A. Omarai, Z. Sadredini, and M. Ebrahimi, "Investigation of the fracture mechanism and mechanical properties of polystyrene/silica nanocomposite in various silica contents", *J. Mater. Sci.*, Vol. 46, pp. 5628-5638, 2011.
- [13] A. Masa, R. Saito, H. Saito, T. Sakai, A. Kaesaman, and N. Lopattananon, "Phenolic resin-crosslinked natural rubber/clay nanocomposites: Influence of clay loading and interfacial adhesion on strain-induced crystallization behavior", *J. Appl. Polym. Sci.*, Vol. 133, pp. 43214, 2016.
- [14] K. P. Sau, T. K. Chaki, and D. Khastgir, "Carbon fibre filled conductive composites based on nitrile rubber (NBR), ethylene propylene diene rubber (EPDM) and their blend", *Polymer*, Vol. 39, pp. 6461-6471, 1998.
- [15] G. K. White, "Thermal expansion of reference materials: copper, silica and silicon", *J. Phys. D Appl. Phys.*, Vol. 6, pp. 2070-2078, 1973.
- [16] S. Choi, J. Park, E. Jeong, B. J. Kim, S. Y. Son, J. M. Lee, J. S. Lee, H. J. Jo, J. Park, and Y. C. Kang, "Deposition and XPS study of Pb, Zr, and Ti films", *J. Chosun Natural Sci.*, Vol. 7, No. 3 pp. 183-187, 2014.
- [17] A. U. Alam, M. M. R. Howlader, and M. J. Deen, "Oxygen plasma and humidity dependent surface analysis of silicon, silicon dioxide and glass for direct wafer bonding", *ECS J. Solid State Sc.*, Vol. 2, pp. P515-P523, 2013.